Modeling creeping flow through a closed crack with a self-affine geometry and an extension to permeability of cracked media

Vladislav A. Yastrebov[1], Guillaume Anciaux[2], Andrei G. Shvarts[1],
Jean-François Molinari[2] and Georges Cailletaud[1]

[1]MINES ParisTech, PSL Research University, Centre des Matériaux, CNRS UMR 7633, Evry, France
email: vladislav.yastrebov, andrei.shvarts, georges.cailletaud@mines-paristech.fr
[2]Laboratoire de Simulations en Mécanique des Solides (LSMS), Ecole Polytechnique Fédérale de Lausanne, GC Station 18, Lausanne, Switzerland
email: guillaume.anciaux, jean-francois.molinari@epfl.ch

ABSTRACT

To model a creeping flow through closed cracks in cracked materials we study a normal mechanical contact between two elastic half-spaces with rough surfaces is studied. The roughness is modeled using a filtering technique in Fourier space: the root mean squared roughness, the spectral content and the fractal dimension are prescribed. The non-linear contact problem is solved using a spectral boundary element method. A general transmissivity laws for incompressible fluid linking roughness parameters and applied load are deduced up to the percolation limit. In this analysis it is assumed that hydrostatic pressure is much smaller than contact pressures. It is shown that the transmissivity decreases exponentially with the effective contact area, which in turn grows linearly with the contact pressure. The effective contact area includes both contact clusters and zones of trapped fluid. A strongly coupled problem of trapped fluid in the wavy contact interface is also considered for compressible and incompressible fluid. The influence of the trapped fluid on the friction angle is studied.

INTRODUCTION

The transport of fluids in geomaterials plays an essential role in many natural geophysical phenomena as well as in geotechnical engineering [Sahimi, 2011]. Apart from the classical porosity geomaterials can contain dense networks of penetrating cracks or fracture porosity. At macroscopic scale these crack increase significantly the permeability of rocks by creating dominant paths through the rock's bulk. Thus the account for the fluid transport through these cracks is essential for many phenomena and applications dealing with fractured porous rocks.

As all engineering and natural surfaces, crack faces are rough and thus when pressurized they form mechanical contact only on a small portion of the nominal contact area, the remaining non-contacting area allows fluid to pass through the crack.

Under increasing normal pressure the true contact area increases leaving lesser space to fluid to pass through the contact interface. When the true contact area reaches the percolation limit which is of about 40%, the flow through the interface stops. To study transmissivity of cracks, we start with a contact problem between two elastic half-spaces brought in mechanical contact by a pressure applied at infinity. Assuming that material of both sides is the same, the effective elastic modulus [Johnson, 1987] is given by $E^* = E/2(1-\nu^2)$, where E and ν are Young's modulus and Poisson's ratio of the rock, respectively. The effective roughness of the crack interface is given by $z^*(x, y) = z_1(x, y) - z_2(x, y)$, where z_1, z_2 are roughness of two half-spaces.

First, we show how the effective periodic rough surface is generated for a given spectral content, a root mean squared height and a fractal dimension (or a Hurst exponent). The method is also generalized for generation of porous media. Second, we show the results of mechanical contact simulation using the spectral boundary element method on the evolution of the contact area and the free volume under increasing contact pressure. After that, on the free volume maps using a finite element method we compute the evolution of transmissivity of the contact interface under increasing load, i.e. we solve Reynolds equation for a viscous incompressible fluid flow between immobile walls. All these results are obtained under the assumption that hydrostatic fluid pressure is much smaller than contact pressure, which has a rather limited use in poromechanics. Finally, we briefly discuss the role of trapped fluid by analyzing a fully coupled problem of a compressible and incompressible fluid trapped in contact

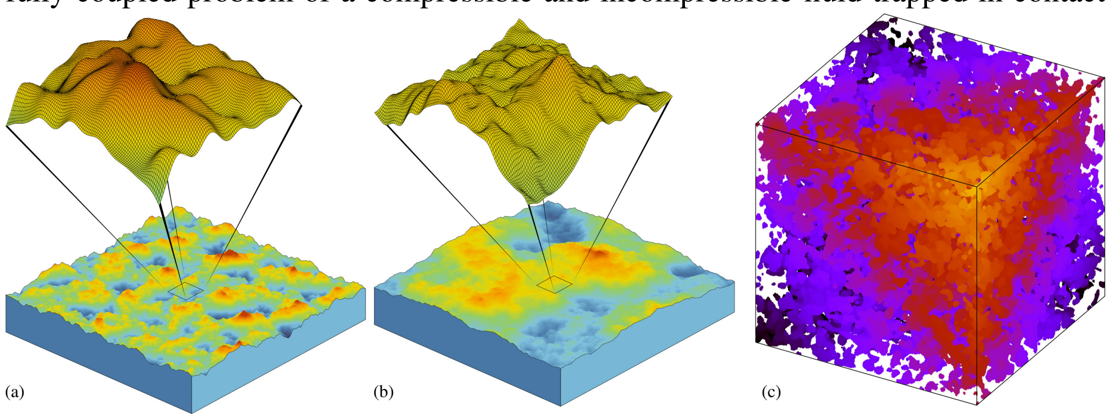

Figure 1. (a-b) Synthetic rough surfaces and zoom on a small portion of the surface ($0.1L \times 0.1L$) with visible discretization grid; (a) $\tilde{k}_l = 4$, $\tilde{k}_l = 64$, $\alpha \approx 12.3$, $H = 0.8$; (b) $\tilde{k}_l = 1$, $\tilde{k}_l = 128$, $\alpha \approx 311.7$, $H = 0.8$; (c) generated porous medium with $256^3 \approx 17 \cdot 10^6$ voxels, only pores are shown.

CRACK ROUGHNESS

Roughness is generated using an FFT filtering technique [Hu and Tonder, 1992]. We generate a white noise $w(x, y)$, $x, y \in [0, L]$ with $\langle w \rangle = 0$, which is transformed in Fourier space $\hat{w} = \mathrm{FFT}(w)$, root mean squared (rms) height $\sqrt{\langle w^2 \rangle}$ is chosen such that $\langle \hat{w}\hat{w}^* \rangle = \Phi_0$. In Fourier space a filter $\hat{f}(k_x, k_y)$ is created, which retains wavenumbers only within frequency band $k \in [k_l, k_s]$, where $k = \sqrt{k_x^2 + k_y^2}$ and k_l, k_s are cutoff wavenumbers for long and short wavelengths, respectively. Within this frequency band, the filter decays as a power law of wavenumber: $\hat{f} = (k/k_l)^{-(H+1)}$, where $H \in (0, 1)$ is the Hurst exponent, which for a fractal surface determines the fractal dimension $D_f = 3 - H$. Taking a product between the white noise in Fourier space and the filter gives the FFT of the resulting roughness $\hat{z} = \hat{w} * \hat{f}$, which is transformed back into real space $z = \mathrm{FFT}^{-1}(\hat{z})$. The power spectral density (PSD) of the surface, which can be found as the Fourier transform of the autocorrelation function follows approximately the power law $\Phi(k) \approx \Phi_0(k/k_l)^{-2(H+1)}$. Such a technique results in an isotropic and Gaussian rough surface, smooth at frequencies higher than k_s: the bigger the product Lk_l (where L is the surface period), the closer the height distribution to a Gaussian one. Such a surface can be studied using a stationary random process model [Nayak, 1971]. An anisotropic roughness, often encountered in fracture surfaces [Ponson et al., 2006], can be also generated using this approach using an anisotropic filter. Geometrical characteristics of the surface can be found through spectral moments m_p of the surface spectrum: rms height $\sqrt{\langle z^2 \rangle} = \sqrt{m_0}$ and rms gradient $\sqrt{\langle |\nabla z|^2 \rangle} = \sqrt{2m_0}$, another important characteristics is the so-called Nayak's parameter $\alpha = m_0 m_4 / m_2^2$. For an isotropic surface spectral moments are given by $m_p = T(p) \int_{-\infty}^{\infty} k^{p+1} \Phi(k)\, dk$, where $T(p) = \int_0^{2\pi} \cos^p(\phi)\, d\phi$. Synthetic rough surfaces are presented in Fig. 1(a-b).

Generation of porous microstructures. It is worth noting that the same technique can be employed for generation fractal-like (self-affine) porous microstructures. The only difference is that all quantities should be defined in three-dimensional space. Starting again with a white noise $w = w(x, y, z)$ centered at zero, one can create a filter in Fourier space $\hat{f} = (k/k_l)^{-(H+1)}$, where in general case $k = \sqrt{(k_x/a)^2 + (k_y/b)^2 + (k_z/c)^2}$, where adimensional parameters a, b, c can be used to produce anisotropic pore distribution. After taking a product of white noise with a filter in Fourier space and returning to real space we obtain a three dimensional function $G(x, y, z) = \mathrm{FFT}^{-1}(\hat{f} * \hat{w})$, by introducing a threshold G_0 we split the bulk $x, y, z \in [0, L]$ into pores for $G > G_0$ and into a bulk material $G \le G_0$. The resulting porosity is given by $\rho_0 = \int_V H(G - G_0) dV / L^3$, where $H(x)$ is the Heaviside function. Note that $G_0 = 0$ corresponds to $\rho_0 = 50\%$ giving the percolation limit for this self-affine Gaussian porosity, negative values of G_0 corresponds to non-penetrating porosity. If a non-uniform threshold is used $G_0 = G_0(x, y, z)$ a non-uniform porosity can be synthesized. An example of isotropic porosity generated using this technique is shown in Fig. 1(c).

MECHANICAL CONTACT BETWEEN CRACK FACES

Under increasing pressure applied at infinity, two elastic half spaces with rough surfaces come in intimate contact at discrete zones forming the true contact area

A; since we consider a periodic roughness the nominal contact area per period is $A_0 = L^2$ and the true contact area can be considered also only within this period. For a crack, since the area of both crack faces is the same, the nominal contact area A_0 is simply a half of the total crack's surface. Moreover, in most situations crack faces form a conformal interface, so at the macro-scale the closed crack is similar to two nominally flat surfaces in contact [Greenwood and Williamson, 1966]. The remaining non-closed gap between two surfaces $g(x, y) > 0$ determines the free volume available for a fluid to go through the contact interface. We first map an elastic contact between two rough half-spaces to an equivalent problem of contact between a rigid surface with an effective roughness z^* with an elastic half-space with an effective elastic modulus E^* [Johnson, 1987]. This problem is solved using a spectral boundary element method [Stanley and Kato, 1997] and an adapted conjugate gradient solver [Polonsky and Keer, 1999]. The external pressure is applied within approximately 100 steps until the true contact area reaches 50% fraction. The non-linear evolution of the contact area depends on the external (nominal) pressure p_0, rms surface gradient $\sqrt{2m_2}$ and Nayak's parameter α: the normalized adimensional nominal pressure is given by $p' = p_0/(\sqrt{2m_2}E^*)$, so the contact area evolves as $A/A_0 = F(p', \alpha)$. Note that F is a non-linear function, but as $p' \to 0$ for an any α the ratio F/p' tends to a unique constant $F/p' \to \sqrt{2\pi}$ [Bush et al., 1975, Carbone and Bottiglione, 2008]. The need in heavy numerical simulations comes from a strong non-linearity of contact problems and from long-range elastic interactions. All available analytical models, both asperity based [Bush et al., 1975, Greenwood, 2006, Carbone and Bottiglione, 2008] and Persson's model [Persson, 2001, Manners and Greenwood, 2006] are unable to predict accurately the contact area evolution [Yastrebov et al., 2015]. Apart from the true contact area that does not conduct any flow, an effective area A_{eff} can be introduced which includes the true contact area and the trapped non-contact area A_{tr}, which also cannot conduct any fluid, giving $A_{\text{eff}} = A + A_{\text{tr}}$. Evidently the transmissivity properties of the crack are determined by this effective non-conducting area. We demonstrate that contrary to the true contact area $A(p')$, the effective area evolves linearly with the nominal pressure up to high area fractions of $30 - 40\%$.

VISCOUS FLOW SIMULATION THROUGH CLOSED CRACKS

Free volume field $g(x, y)$ obtained in mechanical contact simulation for a given nominal pressure p_0 is used to estimate the transmissivity of the contact interface: $K = -Q/\Delta p$, where $Q = \langle q_x \rangle$ is the average flux, q_x is the flux in the direction of the applied pressure drop $\Delta p = p_o - p_i$, where p_o, p_i are the outlet and inlet pressures applied at $x = L$ and x_0, respectively. Periodic boundary conditions are used on lateral sides $y = 0$ and $y = L$ of the simulation domain: $q_y(x, L) = q_y(x, 0)$. The problem of the viscous incompressible fluid flow through a thin interface can be solved using Reynolds equation for immobile walls $\nabla \cdot [g^3(x, y)\nabla p(x, y)/12\mu] = 0$, where μ is pressure insensitive dynamic viscosity of the fluid. Equivalently, an effec-

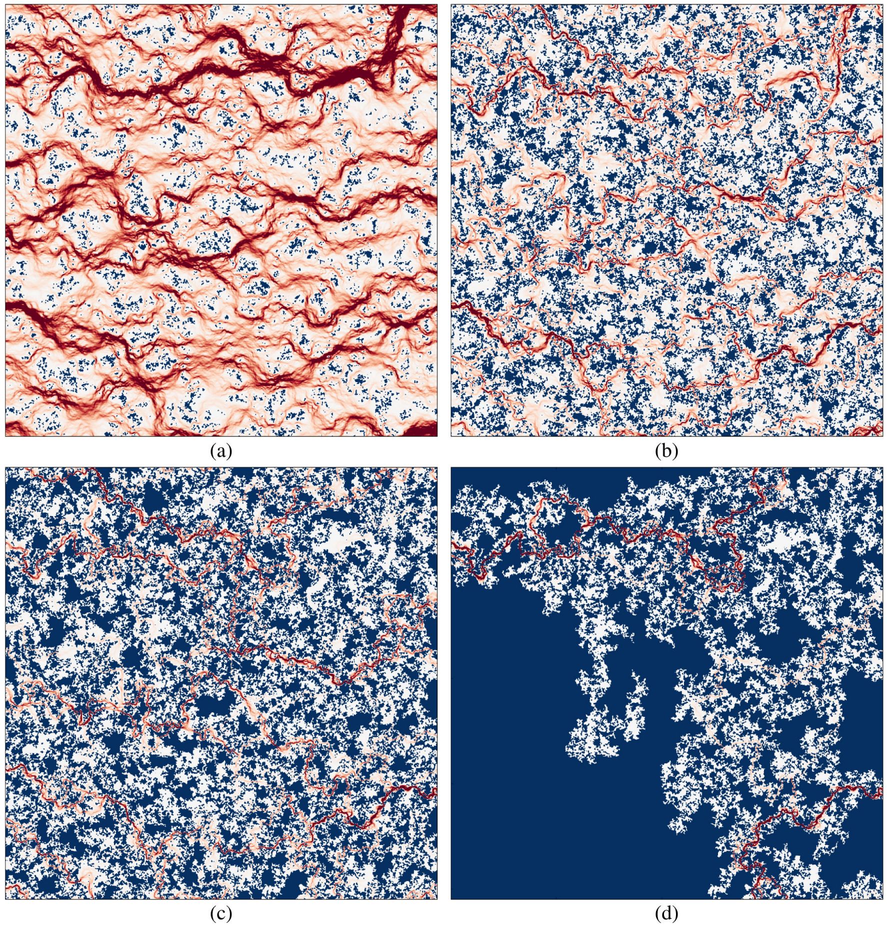

Figure 2. Simulation of the creeping flow through the contact interface at different nominal pressures (a-d): dark uniform-color zones (navy color in online version) represent non-conducting zones A_{eff} including contact clusters and non-contact zones surrounded by contact zones (trapped fluid), gray-scale channels (reddish colors in online version) represent scaled fluid flux $|q|$; inlet and outlet hydrostatic pressures are applied on the left and right sides of the simulation square domain; periodic boundary conditions on lateral borders are used.

tive medium theory can be used [Stroud, 1975, Dapp and Müser, 2016] but with modified in a way that it accounts for non-conducting trapped area A_{tr}. Reynolds equation is solved on a regular grid using the finite element method and a coloring technique to exclude all non-conducting areas A_{eff}, an example of simulation results is depicted in Fig. 2 showing the flux and the effective non-conducting clusters. The simulations demonstrate that the transmissivity decays exponentially with the effective contact area $K \sim \exp(-\gamma A_{\text{eff}}/A_0)$ down to the percolation limit. This result however holds only for weakly interacting solid and fluid, i.e. in the case when the hydrostatic pressure in the fluid in much smaller than contact pressures. Otherwise, a more elaborated coupling scheme is needed, in which the fluid pressure is taken into account in the contact problem. This, however, cannot be ensured in the spectral method, in which the gradient of the hydrostatic pressure over long spatial lengths is hard to take into account.

Generalization to permeability of a system of cracks The approach can be generalized for a representative volume element (RVE) $L \times L \times L$ containing numerous end-to-end flat cracks [Singhal and Gupta, 2010]. Assuming the RVE is subject to the macroscopic stress tensor $\boldsymbol{\Sigma}$, the nominal pressure on every crack can be found as $p_0 = -\boldsymbol{n} \cdot \boldsymbol{\Sigma} \cdot \boldsymbol{n}$, where $\boldsymbol{n}$ is the normal to the crack interface. Knowing the crack dimensions, roughness parameters and the pressure gradient, the flux through a single crack can be found as $\boldsymbol{Q} = -K[\exp(-\gamma A_{\text{eff}}(p_0)/A_0)] \sum_i \Delta p_i \boldsymbol{e}_i L_{oi}/L_i$, where $\boldsymbol{e}_i$ are the unit basis vectors $i = 1 \dots 3$, L_i is the crack length along $\boldsymbol{e}_i$ and L_{oi} is the mean crack width. Summing up contributions from differently oriented cracks the effective permeability tensor depending on crack orientations and macroscopic stress state can be found $\boldsymbol{K}(\boldsymbol{\Sigma})$.

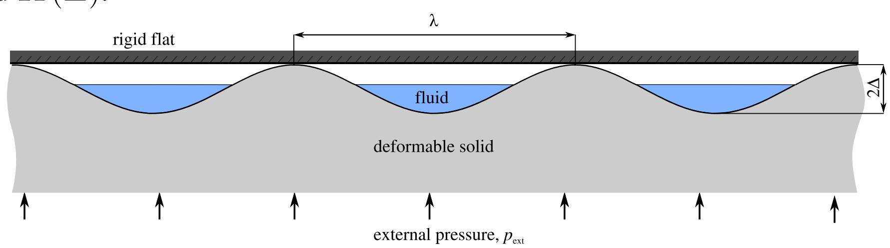

Figure 3. Fluid trapped in the contact interface: a periodic wavy profile of an elastic half-space brought in contact with a rigid flat by an external pressure, a compressible fluid depicted in blue is trapped between contact lines.

TRAPPED FLUID IN CONTACT INTERFACE

A more relevant problem for poromechanics is when the fluid is trapped in the contact interface and the pressure developed in the fluid is fully transmitted to the solid. We considered a simple plane-strain problem (see Fig. 3) for a linearly-elastic solid with a sine-wavy surface $z(x) = \Delta \sin(2\pi x/\lambda)$ brought in mechanical contact with a rigid flat and containing a certain amount of fluid (linear fluid density, i.e. sectional area is $A_f = f\Delta\lambda$), the remaining volume is filled with a much more compressible fluid and is not taken into account. This situation corresponds to an unsaturated porous medium. Up to a certain pressure the system behavior is equivalent to a classical Westergaard problem with a known analytical solution [Westergaard, 1939]: for a given external pressure p_{ext} the contact area and the contact pressure distribution are known. For a certain pressure, the fluid comes in contact too and is pressurized: if the fluid is assumed incompressible, its volume remains constant under increasing load; for a compressible fluid a linear relation between volume and pressure are assumed. This coupled problem can be formulated as an optimization problem under specific constraints for the contact part (contact pressure is not smaller than fluid pressure and the gap is non-negative) and for the fluid part (gap volume is not smaller than fluid volume and fluid pressure is non-negative). Formulated within a monolithic weak form using either the method of Lagrange multipliers or the penalty method (in the case of compressible fluid) to threat inequality constraints, this problem was solved using the finite element method. The details of implementation can be found in [Shvarts and Yastrebov, 2017]. It was shown that if the compressibility modulus of the fluid is greater than this of the solid, then the fluid will eventually open the contact interface. This important result, appearing naturally in the finite element model, cannot emerge within the boundary element framework, in which surface slopes are inherently assumed to be infinitesimal $\Delta/\lambda \ll 1$, see e.g. results of [Kuznetsov, 1985]. The opening of the contact zone by the pressurized fluid results in the decreasing of the macroscopic static coefficient of friction down to zero μ_{gl}, which might also explain the cap in the yield surface of geomaterials [Resende and Martin, 1985].

CONCLUSION

In this short paper we presented a scheme for analyzing the permeability of a representative volume element of a fractured rock subject to an arbitrary stress state. The method is based on phenomenological equations based on results of numerical simulations of the normal mechanical contact for generated self-affine rough crack surfaces and the subsequent finite element solution of Reynolds equation for a creeping flow through the crack interface. In addition a method for generation of volumetric porous media was suggested inspired by the technique used to generate random self-affine surfaces based on the white-noise filtering in Fourier space. Finally, a strongly coupled problem for an almost incompressible fluid trapped in the contact interface was addressed in the framework of the finite element method. The main reported result is that in partly saturated crack under increasing external pressure the fluid should eventually open the trap, which would result in a lowering of macroscopic static friction.

Acknowledgment. VY, AS, GC acknowledge the financial support from MINES ParisTech (Thèse-Open) and Safran Tech. Enriching discussions and help of Julien Vignollet are greatly appreciated.

REFERENCES

[Bush et al., 1975] Bush, A. W., Gibson, R. D., and Thomas, T. R. (1975). The elastic contact of a rough surface. *Wear*, 35(1):87–111.

[Carbone and Bottiglione, 2008] Carbone, G. and Bottiglione, F. (2008). Asperity contact theories: Do they predict linearity between contact area and load? *J Mech Phys Solids*, 56:2555–2572.

[Dapp and Müser, 2016] Dapp, W. B. and Müser, M. H. (2016). Fluid leakage near the percolation threshold. *Scientific reports*, 6.

[Greenwood, 2006] Greenwood, J. A. (2006). A simplified elliptic model of rough surface contact. *Wear*, 261:191–200.

[Greenwood and Williamson, 1966] Greenwood, J. A. and Williamson, J. B. P. (1966). Contact of nominally flat surfaces. *P Roy Soc Lond A Mat*, 295:300–319.

[Hu and Tonder, 1992] Hu, Y. Z. and Tonder, K. (1992). Simulation of 3-D random rough surface by 2-D digital filter and fourier analysis. *Int J Mach Tool Manu*, 32:83–90.

[Johnson, 1987] Johnson, K. L. (1987). *Contact mechanics*. Cambridge University Press.

[Kuznetsov, 1985] Kuznetsov, Y. A. (1985). Effect of fluid lubricant on the contact characteristics of rough elastic bodies in compression. *Wear*, 102(3):177–194.

[Manners and Greenwood, 2006] Manners, W. and Greenwood, J. A. (2006). Some observations on persson's diffusion theory of elastic contact. *Wear*, 261:600–610.

[Nayak, 1971] Nayak, P. R. (1971). Random process model of rough surfaces. *J Lubr Technol (ASME)*, 93:398–407.

[Persson, 2001] Persson, B. N. J. (2001). Theory of rubber friction and contact mechanics. *J Chem Phys*, 115:3840–3861.

[Polonsky and Keer, 1999] Polonsky, I. and Keer, L. (1999). A numerical method for solving rough contact problems based on the multi-level multi-summation and conjugate gradient techniques. *Wear*, 231(2):206–219.

[Ponson et al., 2006] Ponson, L., Bonamy, D., Auradou, H., Mourot, G., Morel, S., Bouchaud, E., Guillot, C., and Hulin, J. P. (2006). Anisotropic self-affine properties of experimental fracture surfaces. *Int J Fracture*, 140(1):27–37.

[Resende and Martin, 1985] Resende, L. and Martin, J. B. (1985). Formulation of Drucker-Prager cap model. *Journal of Engineering Mechanics*, 111(7):855–881.

[Sahimi, 2011] Sahimi, M. (2011). *Flow and transport in porous media and fractured rock: from classical methods to modern approaches*. John Wiley & Sons.

[Shvarts and Yastrebov, 2017] Shvarts, A. G. and Yastrebov, V. A. (2017). The effect of trapped fluid in a wavy contact interface. *in preparation*.

[Singhal and Gupta, 2010] Singhal, B. B. S. and Gupta, R. P. (2010). *Applied hydrogeology of fractured rocks*. Springer Science & Business Media.

[Stanley and Kato, 1997] Stanley, H. M. and Kato, T. (1997). An FFT-based method for rough surface contact. *J Tribol-T ASME*, 119:481–485.

[Stroud, 1975] Stroud, D. (1975). Generalized effective-medium approach to the conductivity of an inhomogeneous material. *Physical Review B*, 12(8):3368.

[Westergaard, 1939] Westergaard, H. M. (1939). Bearing pressures and cracks. *J Appl Mech (ASME)*, 6:49.

[Yastrebov et al., 2015] Yastrebov, V. A., Anciaux, G., and Molinari, J.-F. (2015). From infinitesimal to full contact between rough surfaces: evolution of the contact area. *International Journal of Solids and Structures*, 52:83–102.